The effect of growth time and oxygen flow on the properties of electrochromic WO₃ thin layers grown by LPCVD

D. Louloudakis[1]*, D. Vernardou[1,2], G. Papadimitropoulos[3], D. Davazoglou[3] and E. Koudoumas[1,2]*

[1]Center of Materials Technology and Photonics, School of Engineering, Technological Educational Institute of Crete, 710 04 Heraklion, Crete, Greece

[2]Department of Electrical Engineering, School of Engineering, Technological Educational Institute of Crete, 710 04 Heraklion, Crete, Greece

[3]NCSR "Demokritos", Institute of Nanoscience and Nanotechnology, P.O. Box 60228, 15310 Agia Paraskevi, Athens, Greece

*Corresponding authors

Abstract

Results are presented regarding the development of functional electrochromic WO₃ thin layers, using a simple, one step and fast process without the need of template or seed layers or even post-annealing, factors favoring large scale industrial deposition. In particular, low pressure chemical vapor deposition (LPCVD) was employed to develop ɤ-monoclinic WO₃ crystalline phase of granular agglomerations structure, with a thickness from 60 nm up to 160 nm onto FTO coated glass substrates. The effect of growth time and oxygen flow on the structural, morphological and electrochemical properties of WO₃ thin layers was investigated. It was found that a deposition time of 15min and an O_2 flow rate through the reactor of 0.1 l/min result in a more stable behavior during the interchange charge circles. Copyright © 2018 VBRI Press.

Keywords: ɤ-monoclinic WO₃; electrochemical response.

Introduction

Electrochromic windows have attracted a lot of interest since they can offer controlled modulation of the transmission in a broad spectral range. Compared with other chromic materials, such as photochromic and thermochromic windows, the development of electrochromic windows is complex requiring full device configuration and electric supply, while, at the same time, they must meet particular requirements for architectural window applications. In general, an electrochromic window requires transparent conductors, electrolyte, and charge storage materials, they should be highly transparent to visible light at the bleached state, and must have appropriate refractive index to minimize reflections. In addition, practical applications require solid-state electrolytes, such as polymer ion gels or ion-conducting ceramics, in order to avoid problems coming from the use of liquid electrolytes, like leaks, fire, or even deformation/breaking of the glass, especially for large window applications.

The mostly used electrochromic devices are based on a thin-film battery-type configuration. A layer of electrochromic material (i.e. metal oxide) is deposited on a Transparent Conductive Electrode (TCO) working electrode, while a charge storage layer is deposited onto a TCO counter electrode. These two electrodes are joined by a layer serving as an ion-conducting electrolyte and separator. Such a device, which is initially transparent, becomes dark when ions are inserted into the electrochromic layer, and it bleaches when the ions are extracted, the magnitude of the color change directly depended on the amount of the inserted charge. These devices exhibit open circuit memory and can maintain a colored state for an extended period of time.

Transition metal oxides are normally quite effective as electrochromic layer in electrochromic devices, especially if one considers their capability to present considerable variations in stoichiometry, and the ease in their deposition in form of thin films, which is required for device manufacturing. Tungsten oxide (WO₃) has been extensively investigated due to its appreciable electrochromic properties in the visible and infrared region, exhibiting large optical modulation, good durability, low power consumption, less stress for the viewer's eyes, and relatively low price [1]. Electrochromic WO₃ thin films have been deposited by a large number of techniques, including thermal evaporation, electrodeposition, spray pyrolysis, chemical vapor deposition, electron beam evaporation, magnetron sputtering, sol-gel etc. [2 - 13]. Among these techniques, chemical vapor deposition (CVD) can offer

ease control on the properties of the films, through the growth conditions, can be easily integrated to float-glass lines and offers fast deposition rate.

In this work, we employed a simple, one step and fast process without the use of template or seed layers or even post-annealing, factors favoring large scale industrial deposition, for the growth of ɤ-monoclinic WO_3 layers on fluorine doped tin dioxide (FTO) glass substrates, exhibiting significant electrochemical behavior. The influence of the deposition time and the oxygen flow, at a constant temperature, on the basic characteristics as well as on the electrochemical response of the WO_3 layers was examined, in a trial to optimize their performance in smart window applications.

Experimental conditions

Materials

The WO_3 layers were grown onto FTO coated glass substrates by LPCVD, the respective procedure described in details elsewhere [14,15]. For the scopes of this work, the following conditions were employed: (i) precursor tungsten hexacarbonyl ($W(CO)_6$), (ii) substrate temperature 530 °C, (iii) flow of N_2 carrier gas 0.05 liters/min, (iv) deposition times 10, 15 and 20 minutes and (v) flows of O_2 within the reactor 0.05, 0.075 and 0.1 liters/min. These deposition parameters resulted in layer thicknesses of about 60 up to 160 nm.

Characterization

Structural analysis was performed in a Siemens D5000 Diffractometer using operating conditions: CuKα ($\lambda = 1.54056$ Å), 2θ= 20.0-50.0º, step time 60 s/º and a Nicolet Almega XR micro-Raman system for a range of 100-1000 cm^{-1} and a laser line at 473 nm. The morphology of the samples was examined in a Jeol JSM-7000F field-emission scanning electron microscope (FE-SEM) at an operating voltage of 15 kV. All samples were over-coated with a thin of gold prior to FE-SEM analysis to avoid charging. Electrochemical measurements were performed using a three-electrode cell as reported previously [14-17]. The measurements were accomplished using a scan rate of 10 mV s^{-1} through the voltage range of -1000 mV to +1000 mV. The area of the working electrode (working electrode refers to the WO_3 layer grown on FTO) exposed to the electrolyte was 1 cm^2. The lithium ion intercalation/de-intercalation process with respect to time was also studied using chronoamperometry at -1000 mV and +1000 mV for a step of 200 s and a total time period of 2000 s.

Results and discussion

Initially, WO_3 samples were deposited for various growth times, keeping the deposition temperature constant at 530°C, a value chosen following previous studies, and an oxygen flow of 0.1 liters/min. All as-grown WO_3 layers were transparent and adherent passing the Scotch tape test (removal of an X shaped piece of sticking tape [18]).
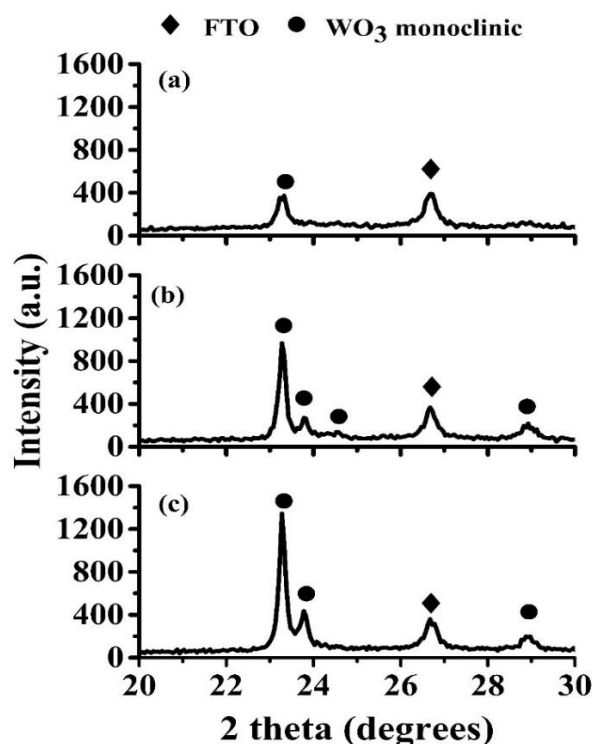
Fig. 1. XRD patterns of WO_3 layers grown by LPCVD for: (a) 10, (b) 15 and (c) 20 min.

Fig. 1 shows the X-ray diffraction (XRD) patterns of WO_3 layers grown for 10, 15 and 20 minutes onto FTO coated glass substrates. As shown in Fig. 1a, for a growth time of 10 min, a characteristic peaks at 23.3º of the ɤ-monoclinic WO_3 crystalline phase, corresponding to (002) crystalline orientation, is observed [19-21]. Longer deposition times (**Fig. 1b and 1c**) lead to additional contributions at 23.8º, 24.6º and 29º coming from the (020), (200) and (112) crystalline orientations of the same ɤ-monoclinic crystalline phase. Moreover, as the deposition time increases, the peaks become more intense and narrow, indicating an improvement of crystallinity. At the same time, the higher intensity of the (002) peak in the XRD spectrum suggests a preferential orientation perpendicular to the thin film plane, i.e. along the c-axis. Finally, in all XRD patterns, the reflection due to the FTO glass substrate at 26.5º with respective Miller indices (110) was also observed [22]. Missing peaks of ɤ-monoclinic crystalline phase may be attributed to the fact that layers have a thickness around 100nm.

At room temperature, ɤ- monoclinic WO_3 is the most common and stable phase, consisting of planar arrays of corner-sharing WO_6 octahedra, placed perpendicular to the [001] hexagonal axis and held together along the z axis by Van de Waal's forces. In this structural configuration, the site of the missing cation B (compared to a perovskite-like atomic configuration with the ideal ABO3 cubic crystal structure) is empty and easily accessible through tunnels present between the octahedra, thus allowing for ionic transport and intercalation within the structure in case of an external force and leading in a layer with excellent electrochromic response.
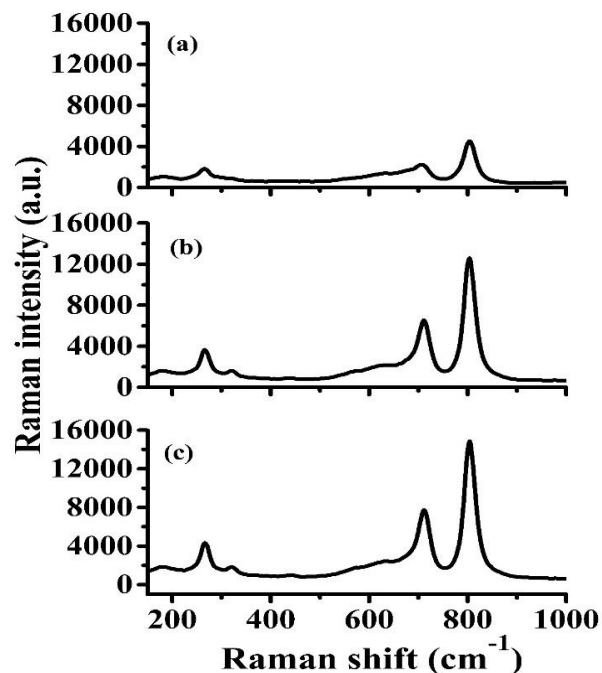
Fig. 2. Raman spectra of WO$_3$ layers grown by LPCVD for: (a) 10, (b) 15 and (c) 20 min.

Raman spectroscopy also confirmed the presence of monoclinic WO$_3$ phase for the layers grown for times $\geq$ 10 min [23]. **Fig. 2** displays the Raman spectra of WO$_3$ for the three samples discussed earlier. Raman peaks at the frequencies of 269 and 323 cm^{-1} are assigned the W-O-W bending modes of bridging oxide ions [23], while the W-O-W stretching mode (tungsten oxide network) corresponds to the high frequency Raman peaks at 713 and 806 cm^{-1} [24]. Increasing deposition time was observed to result in both stronger and narrower peaks, another evidence of the improvement of the crystallinity.

FE-SEM analysis of the as-grown WO$_3$ layers is shown in **Fig. 3**. In all cases, the layers showed a granular structure packed in agglomerations of grains. As the growth time increases and the film crystallinity is improved, a decrease of grains size within the agglomerations can be observed, the surface presenting at the same time a more porous appearance. For a deposition time of 20 min or larger, the morphology of the grains was changed, these presenting a flower-like appearance. The 3D morphology is expected to be quite effective regarding electrochromic applications, since this presents more available places for the intercalation and the de-intercalation of Li ions [25,26].

In order to study the effect of the growth time, and the subsequent structural and morphological characteristics, on the electrochemical performance of the as-grown WO$_3$ layers, cyclic voltammogram curves were collected using a scan rate of 10 mV s^{-1} and 1 M LiClO$_4$/propylene carbonate as electrolyte and are presented in **Figs. 4a, 4b** and **4c**. All curves are normalized to the geometric area of the working electrode, resulting in units of μA cm^{-2}. The as grown WO$_3$ layers were found to be transparent, while, after the
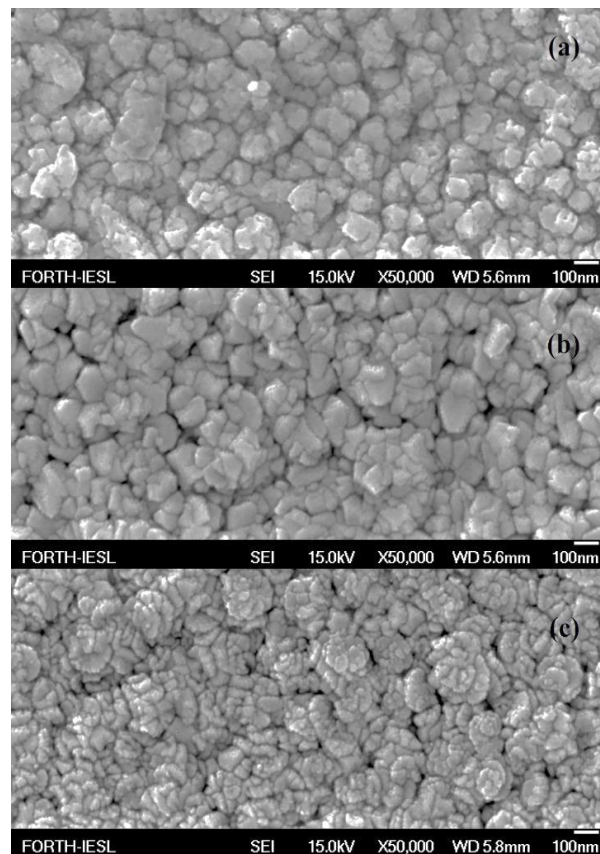

Fig. 3. FE-SEM images of WO$_3$ layers grown by LPCVD for: (a) 10, (b) 15 and (c) 20 min.

intercalation of the Li ions, the color was changed to blue. The layers were becoming again transparent after the de-intercalation of the Li ions, except in some cases where they remained slightly colored, especially after many cycles of intercalation/de-intercalation of Li ions, since some ions were remaining within the WO$_3$ lattice [27, 28]. This color - bleach process can be represented according to the following equation [29]:

$$WO_3 \text{ (transparent)} + xLi^+ + xe^- \leftrightarrow Li_xWO_3 \text{ (blue)}$$
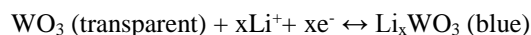
The results shown in **Fig. 4**, can be summarized as following:
(a) the samples grown for 10 min present quite low current and charge, these being significantly reduced after the first scan, due to the dissolution and the fast degradation of the respective layer (**Fig 4a**);
(b) the samples grown for 15 (**Fig. 4b**) and 20 min (**Fig. 4c**) were found to be more stable for up to 500 cycles, presenting however degradation at some extend, indicated by a change in the shape of the curve and a shift of the maxima. This behavior can be attributed to the non-reversibility of the process, leading in permanent presence of Li ions within the WO$_3$ lattice. The sample grown for 15 min appeared to have the best performance, regarding the stability of response, while the higher current/charge was found in the 20 min sample. The maxima appeared around -0,5 V are attributed to the intercalation and

the de-intercalation of the Li+ ions, followed by the gain or the loss of an electron. Moreover, after the de-intercalation of the Li+ ions, the samples were becoming again transparent, at least in the case of up to 250 cycles, while, for even more cycles, some samples remained slightly colored, due to the remaining of Li ions within the WO_3 lattice, as mentioned earlier.

Chronoamperometry tests were also conducted for layers grown for different growth times, switching the voltage between -1000 mV and +1000 mV at an interval of 200 s, the respective curves shown in **Figs. 4d-4f**. The samples grown for 10 min were found to present a significant reduction of the current density with increasing cycle number, as expected following the voltammograms, while the 15 and 20 min samples exhibit a more stable behavior. The respective current density was found to present a rather small reduction up to the 500th cycle, especially in the case of the sample grown for 15 min, which appeared to have a better stability.
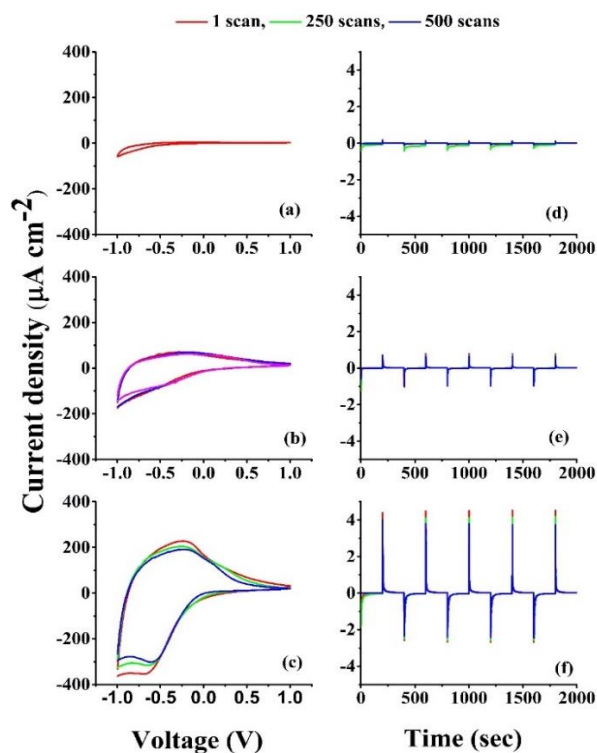
Fig. 4. Cyclic voltammograms of WO_3 layers grown by LPCVD for: (a) 10, (b) 15 and (c) 20 min, collected using a scan rate of 10 mV s⁻¹ and 1 M LiClO₄/propylene carbonate as electrolyte. Chronoamperometry curves of WO_3 layers grown by LPCVD for: (d) 10, (e) 15 and (f) 20 min, switching the voltage between -1 V and +1V at an interval of 200 s.

Then, the amount of Li+ charge interchanged between the layers and the electrolyte was calculated by integration of excess current densities measured for the 1st, the 250th and the 500th cycles, the respective results shown in **Table 1**, together with the intercalation and de-intercalation times. As can be seen, the sample grown for 20 min presents the best performance, regarding the interchanged charge. In all cases, a difference exists

between intercalation and de-intercalation charge, attributed to the small number of ions remaining within the WO_3 lattice. This difference is less significant for the samples grown for 15 and 20 min (27% and 25% respectively), being quite large for the 10 min sample (48%). Moreover, with increasing cycle number, the intercalation and de-intercalation charge appeared to be decreased due to the ageing of the samples, the ageing being less pronounced for the 15 and the 20 min samples. Regarding the intercalation and de-intercalation times, the faster response times were observed in the sample grown for 15 min for all recorded cycles, the 10 and 20 min samples exhibiting similar response times, at least for the 1st cycle. With increasing number of cycles, the 10 min samples appeared to have much slower response, in contrast to the 20 min sample, where the response was becoming faster. Comparing the results of **Table 1**, one can conclude that the WO_3 sample grown for 15 min presents an optimum response, as compared to the other grown samples, although in the 20 min sample, the interchanged charge is much larger.

Table 1. Li+ charge interchanged between the layers and the electrolyte measured for the 1st, the 250th and the 500th cycles and the respective intercalation and de-intercalation times for samples grown for different time periods.

No of cycles	Parameter	10 min	15 min	20 min
1	Intercalation charge (mC cm⁻²)	3.98	6.50	27.77
	De-intercalation charge (mC cm⁻²)	2.08	4.72	18.18
	Intercalation time (sec)	23	15	25
	De-intercalation time (sec)	20	14	19
250	Intercalation charge (mC cm⁻²)	2.13	4.26	21.76
	De-intercalation charge (mC cm⁻²)	0.51	3.17	13.14
	Intercalation time (sec)	55	11	21
	De-intercalation time (sec)	26	10	7
500	Intercalation charge (mC cm⁻²)	0.85	3.87	19.28
	De-intercalation charge (mC cm⁻²)	0.29	2.87	12.49
	Intercalation time (sec)	37	11	18
	De-intercalation time (sec)	23	9	8

The observed behavior seems to be consistent with that already reported in the literature [25,26], since better crystallinity and more porous surface morphology lead to faster and larger Li+ charge interchange as well as better stability of the electrochemical response with increasing number of intercalation and de-intercalation cycles. However, following our results, it seems that when the morphology becomes too porous, although the interchanged charge becomes maximum, the response time is slower and the stability becomes less favorable.
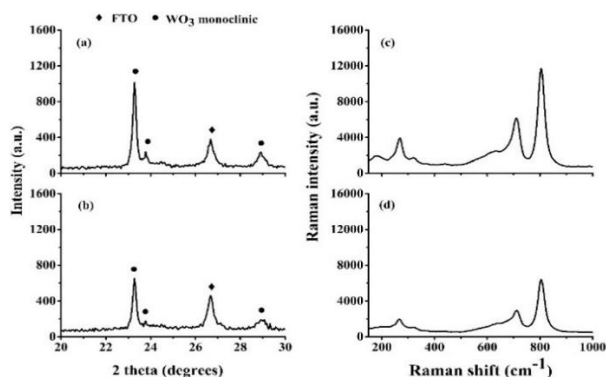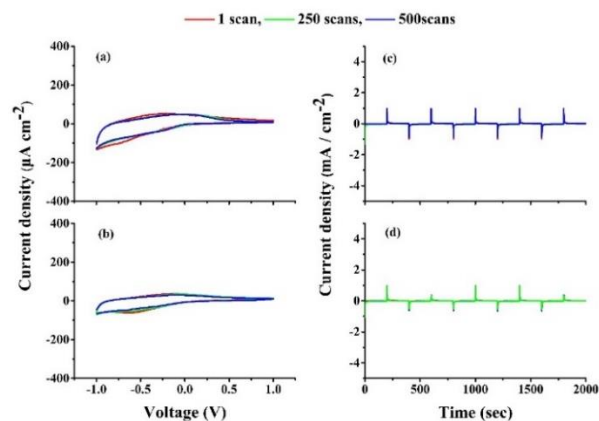
Fig. 5. XRD patterns of WO$_3$ layers grown by LPCVD for an oxygen flow of: (a) 0.05 and (b) 0.075 l/min. Raman spectra of WO$_3$ layers grown by LPCVD for an oxygen flow of: (c) 0.05 and (d) 0.075 l/min.

As a next step, another set of WO$_3$ layers was deposited, employing various oxygen flows, keeping the same deposition temperature of 530°C and a deposition time of 15 min, since this corresponds to the more stable response, for the experimental conditions employed. **Figs. 5a** and **5b** present the X-ray diffraction (XRD) patterns of WO$_3$ layers grown with an oxygen flow of 0.05 and 0.075 l/min onto clean FTO coated glass substrates, the respective pattern of the sample grown with 0.1 l/min shown in **Fig. 1a**. Comparing these results, one can see that decreasing oxygen flow results in a similar XRD pattern, as far as it concerns the positions of the peaks. However, the intensity of the peaks is reduced and these become broader, an indication that the crystallinity is reduced. Similar conclusion can be obtained from the Raman spectra of the samples grown with an oxygen flow of 0.05 and 0.075 l/min, shown in **Figs 5c** and **5d**, where, although the patterns are similar to those recorded for the sample grown with 0.1 l/sec (shown in **Fig. 2a**), their intensity is reduced and they are broader. Regarding an increase of the oxygen flow to values above 0.1 l/s, this did not improve further the crystallinity of the layers. Regarding the FE-SEM analysis of the WO$_3$ layers, these also present a granular structure packed in agglomerations of grains. As the oxygen flow reduces and the film crystallinity is decreased, the layers become smoother, their 3D morphology disappearing.

Cyclic voltammogram curves were then collected using a scan rate of 10 mV s^{-1} and 1 M LiClO$_4$/propylene carbonate as electrolyte and are presented in **Figs. 6a** and **6b,** for the samples grown with an oxygen flow of 0.05 and 0.075 l/min. All of the curves are normalized to the geometric area of the working electrode, resulting in units of μA cm^{-2}. The WO$_3$ layers were found to exhibit similar response to that recorded for an oxygen flow of 0.1 l/min (**Fig. 4a**), the response however being weaker and less stable. Chronoamperometry tests were also conducted, switching the voltage between -1000 mV and +1000 mV at an interval of 200 s, the respective curves shown in **Figs. 6c** and **67d**. As the number of cycle was increasing, the current density was found decreasing, the decrease being more pronounced for smaller oxygen flows.

Table 2. Li$^+$ charge interchanged between the layers and the electrolyte measured for the 1st, the 250th and the 500th cycles and the respective intercalation and de-intercalation times for samples grown for different oxygen flow rates.

No of cycles	Parameter	0.05 l/min	0.075 l/min	0.1 l/min
1	Intercalation charge (mC cm^{-2})	4.69	6.88	6.50
	De-intercalation charge (mC cm^{-2})	3.56	4.57	4.72
	Intercalation time (sec)	21	22	15
	De-intercalation time (sec)	20	18	14
250	Intercalation charge (mC cm^{-2})	3.24	4.90	4.26
	De-intercalation charge (mC cm^{-2})	2.85	3.73	3.17
	Intercalation time (sec)	19	16	11
	De-intercalation time (sec)	12	12	10
500	Intercalation charge (mC cm^{-2})	3.44	3.27	3.87
	De-intercalation charge (mC cm^{-2})	2.20	2.84	2.87
	Intercalation time (sec)	14	14	11
	De-intercalation time (sec)	12	9	9

Fig. 6. Cyclic voltammograms of WO$_3$ layers grown by LPCVD for an oxygen flow of: (a) 0.05 and (b) 0.075 l/min, collected using a scan rate of 10 mV s^{-1} and 1 M LiClO$_4$/propylene carbonate as electrolyte. Chronoamperometry curves for an oxygen flow of: (a) 0.05 and (b) 0.075 l/min, switching the voltage between -1 V and +1 V at an interval of 200 s.

Finally, the amount of Li$^+$ charge interchanged between the layers and the electrolyte was calculated for the 1st, the 250th and the 500th cycles, the respective results shown in **Table 2** together with the intercalation and de-intercalation times. As can be seen, all values are worse than those recorded for the sample grown with 0.1 l/min. Therefore, the WO$_3$ sample grown for 15 min with an oxygen flow of 0.1 l/min presents an optimum

response. For larger oxygen flows, the recorded response was found to be similar to that of the 0.1 l/min case.

Comparing our results with others in the recent literature [5,9,27], one can see the charge density and the coloration/bleaching times of our WO_3 layers, deposited using a simple, one step and fast process without the employment of template or seed layers or even post-annealing, is comparable with others made using more sophisticated routes such as sputtering, their stability during the cycles being quite good.

Conclusions

In this work, the effect of growth time and oxygen flow rate on the structural, morphological and electrochemical characteristics of WO_3 thin layers grown by low pressure chemical deposition was investigated. It was found that layers of ɤ-monoclinic WO_3 crystalline phase, having granular agglomerations structure with thickness from 60 nm to 160 nm can be obtained at a 530°C substrate temperature, for deposition times of 10-20 minutes and oxygen flow rates of 0.05-0.1 l/s. With increasing growth time, the crystallinity was improved and a more porous surface was induced, leading in an improvement of the electrochemical response. Moreover, low oxygen flow rates resulted in less crystalline layers exhibiting less effective electrochemical response. Optimum, fast and stable electrochemical response was found for a deposition time of 15 min and an oxygen flow rate of 0.1 l/s.

References

1. E. S. Lee, D. L. Di Bartolomeo, Application issues for large-area electrochromic windows in commercial buildings, Sol. Energ. Mat. Sol. C., **2002**, 71, 465.
   DOI: 10.1016/S0927-0248(01)00101-5
2. C. G. Granqvist, Electrochromic tungsten oxide films: Review of progress 1993–1998, Sol. Energ. Mat. Sol. C., **2000**, 60, 201.
   DOI: 10.1016/S0927-0248(99)00088-4
3. A. A. Joraid, Comparison of electrochromic amorphous and crystalline electron beam deposited WO_3 thin films, Curr. Appl. Phys., **2009**, 9, 73.
   DOI: 10.1016/j.cap.2007.11.012
4. A. J. More, R. S. Patil, D. S. Dalavi, S. S. Mali, M. G. Gang, J. H. Kim, Electrodeposition of nano-granular tungsten oxide thin films for smart window application, Mater. Lett., **2014**, 134, 298.
   DOI: 10.1016/j.matlet.2014.07.059
5. A. N. Y. Bhosalea, S. S. Malib, C. K. Hongb, A. V. Kadama, Hydrothermal synthesis of WO_3 nanoflowers on etched ITO and their electrochromic properties, Electrochim. Acta, **2017**, 246, 1112.
   DOI: 10.1016/j.electacta.2017.06.142
6. Y. Lee, H. J. Choi, T. Kima, K.-H Hwang, J.-H. Yu, S.-H. Nam, D. H. Ryu, J.-H. Boo, Enhanced efficiency of the honeycomb-structured film WO_3 composed of nanorods for electrochromic properties, Thin Solid Films, **2017**, 637, 14.
   DOI: 10.1016/j.tsf.2017.02.065
7. Y. Li, D. Chen and R. A. Caruso, Enhanced electrochromic performance of WO_3 nanowire networks grown directly on fluorine-doped tin oxide substrates, J. Mater. Chem. C, **2016**, 4, 10500.
   DOI: 10.1039/c6tc03563a
8. M. Gerosa, C. Di Valentin, G. Onida, C. E. Bottani, and G. Pacchioni, Anisotropic Effects of Oxygen Vacancies on Electrochromic Properties and Conductivity of γ‑ Monoclinic WO_3, J. Phys. Chem. C, **2016**, 120, 11716.
   DOI: 10.1021/acs.jpcc.6b02707
9. K. Ghosh, A. Roy, S. Tripathi, S. Ghule, A. K. Singh and N. Ravishankar, Insights into nucleation, growth and phase selection of WO_3: morphology control and electrochromic properties, J. Mater. Chem. C, **2017**, 5, 7307
   DOI: 10.1039/c7tc01714f
10. C. M. Wang, C. Y. Wen, Y. C. Chen, K. S. Kao, D. L. Cheng, C. H. Peng, Effect of Deposition Temperature on the Electrochromic Properties of Electron Beam-Evaporated WO3 Thin Films, Integr. Ferroelectr., **2014**, 158, 62.
    DOI: 10.1080/10584587.2014.957117
11. T. S. Yang, Z. R. Lin, M. S. Wong, Structures and electrochromic properties of tungsten oxide films prepared by magnetron sputtering, Appl. Surf, Sci., **2005**, 252, 2029.
    DOI: 10.1016/j.apsusc.2005.03.170
12. F. Zhang, H. Q. Wang, S. Wang, J. Y. Wang, Z. C. Zhong, Y. Jin, Structures and optical properties of tungsten oxide thin films deposited by magnetron sputtering of WO_3 bulk : Effects of annealing temperatures, Chinese Phys. B, **2014**, 23, 098105.
    DOI: 10.1088/1674-1056/23/9/098105
13. A. P. Baker, S. N. B. Hodgson, M. J. Edilisinghe, Production of tungsten oxide coatings, via sol–gel processing of tungsten anion solutions, Surf. Coat. Tech., **2002**, 153, 184.
    DOI: 10.1016/S0257-8972(01)01673-5
14. K. Psifis, D. Louloudakis, D. Vernardou, E. Spanakis, G. Papadimitropoulos, D. Davazoglou, N. Katsarakis, E. Koudoumas, Effect of O_2 flow rate on the electrochromic response of WO_3 grown by LPCVD, Phys. Status Solidi C, **2015**, 12, 1011.
    DOI: 10.1002/pssc.201510004
15. D. Vernardou, D. Louloudakis, E. Spanakis, N. Katsarakis, and E. Koudoumas, Electrochemical properties of vanadium oxide coatings grown by hydrothermal synthesis on FTO substrates, New J. Chem., **2014**, 38, 1959.
    DOI: 10.1039/C3NJ00931A
16. D. Vernardou, K. Psifis, D. Louloudakis, G. Papadimitropoulos, D. Davazoglou, N. Katsarakis, E. Koudoumas, Low pressure CVD of electrochromic WO_3 at 400°C, Journal of the Electrochemical Society, **2015**, 162, H579
    DOI: 10.1149/2.0281509jes
17. D. Vernardou, M. Apostolopoulou, D. Louloudakis, E. Spanakis, N. Katsarakis, E. Koudoumas, J. McGrath, and M.E. Pemble, Electrochemical properties of opal-V_6O_{13} composites, J. Alloy Compd., **2014**, 586, 621.
    DOI: 10.1016/j.jallcom.2013.10.151
18. T. D. Manning, I. P. Parkin, R. J. H. Clark, D. Sheel, M. E. Pemble, and D. Vernardou, Intelligent window coatings: atmospheric pressure chemical vapour deposition of vanadium oxides, J. Mater. Chem., **2002**, 12, 2936.
    DOI: 10.1039/B205427M
19. X. Hu, Q. Ji, J. P. Hill, and K. Ariga, Large-scale synthesis of WOx–EDA nanobelts and their application as photoswitches, Cryst. Eng. Commun., **2011**, 13, 2237.
    DOI: 10.1039/C0CE00466A
20. H. Zhang, M. Yao, L. Bai, W. Xiang, H. Jin, J. Lin, and F. Yuan, Synthesis of uniform octahedral tungsten trioxide by RF induction thermal plasma and its application in gas sensing, Cryst. Eng. Commun., **2013**, 15, 1432.
    DOI: 10.1039/C2CE26514A
21. Z. Lu, S. M. Kanana, and C. P. Tripp, Synthesis of high surface area monoclinic WO3 particles using organic ligands and emulsion based methods, J. Mater. Chem., **2002**, 12, 983.
    DOI: 10.1039/B107993J
22. E. Elangovan and K. Ramamurthi, Studies on micro-structural and electrical properties of spray-deposited fluorine-doped tin oxide thin films from low-cost precursor, Thin Solid Films, **2005**, 476, 231.
    DOI: 10.1016/j.tsf.2004.09.022

23. M. Boulova and G. Lucazeau, Crystallite Nanosize Effect on the Structural Transitions of WO_3 Studied by Raman Spectroscopy, J. Solid State Chem., **2002**, 167, 425.
   DOI: 10.1006/jssc.2002.9649

24. H. Habazaki, Y. Hayashi, and H. Konno, Characterization of electrodeposited WO_3 films and its application to electrochemical wastewater treatment, Electrochim. Acta, **2002**, 47, 4181.
   DOI: 10.1016/S0013-4686(02)00435-8

25. R. T. Wen, M. A. Arvizu, M. Morales-Luna, C. G. Granqvist and G. A. Niklasson, Ion Trapping and Detrapping in Amorphous Tungsten Oxide Thin Films Observed by Real-Time Electro-Optical Monitoring, Chem. Mater., **2016**, 28, 4670
   DOI: 10.1021/acs.chemmater.6b01503

26. S. Poongodi, P. S. Kumar, Y. Masuda, D. Mangalaraj, N. Ponpandian, C. Viswanathan, S. Ramakrishna, Synthesis of hierarchical WO_3 nanostructured thin films with enhanced electrochromic performance for switchable smart window, RSC Adv., **2015**, 5, 96416.
   DOI: 10.1039/C5RA19177G

27. B. Baloukas, M. A. Arvizu, R-T Wen, G.A. Niklasson, C.G. Granqvist, R. Vernhes, J.E. Klemberg-Sapieha, L. Martinu, Galvanostatic Rejuvenation of Electrochromic WO_3 Thin Films: Ion Trapping and Detrapping Observed by Optical Measurements and by Time-of-Flight Secondary Ion Mass Spectrometry, ACS Appl. Mater. Inter., **2017**, 9, 16995.
   DOI: 10.1021/acsami.7b01260

28. K. Christou, D. Louloudakis, D. Vernardou, C. Savvakis, N. Katsarakis, E. Koudoumas, G. Kiriakidis, Effect of solution chemistry on the characteristics of hydrothermally grown WO_3 for electroactive applications, Thin Solid Films, **2015**, 594 333.
   DOI: 10.1016/j.tsf.2015.03.045

29. C. G. Granqvist, Handbook of Inorganic Electrochromic Materials, Elsevier, New York 1995.